Drug and Chemical Toxicology

ISSN: 0148-0545 (Print) 1525-6014 (Online) Journal homepage: http://www.tandfonline.com/loi/idct20

Effects of titanium dioxide nanoparticles on human keratinocytes

Clayton Wright, Anand Krishnan V. Iyer, Liying Wang, Nianqiang Wu, Juan S. Yakisich, Yon Rojanasakul & Neelam Azad

To cite this article: Clayton Wright, Anand Krishnan V. Iyer, Liying Wang, Nianqiang Wu, Juan S. Yakisich, Yon Rojanasakul & Neelam Azad (2017) Effects of titanium dioxide nanoparticles on human keratinocytes, Drug and Chemical Toxicology, 40:1, 90-100, DOI: 10.1080/01480545.2016.1185111

To link to this article: http://dx.doi.org/10.1080/01480545.2016.1185111

Published online: 16 Jun 2016.

Drug and Chemical Toxicology

www.tandfonline.com/idct
ISSN: 0148-0545 (print), 1525-6014 (electronic)

Drug Chem Toxicol, 2017; 40(1): 90–100
 DOI: 10.1080/01480545.2016.1185111

Taylor & Francis
Taylor & Francis Group

RESEARCH ARTICLE

Effects of titanium dioxide nanoparticles on human keratinocytes

Clayton Wright[1], Anand Krishnan V. Iyer[1], Liying Wang[2], Nianqiang Wu[3], Juan S. Yakisich[1], Yon Rojanasakul[4], and Neelam Azad[1]

[1]*Department of Pharmaceutical Sciences, Hampton University, Hampton, VA, USA,* [2]*Allergy and Clinical Immunology Branch, National Institute for Occupational Safety and Health, Morgantown, WV, USA,* [3]*Department of Mechanical & Aerospace Engineering, and* [4]*Department of Pharmaceutical and Pharmacological Sciences, West Virginia University, Morgantown, WV, USA*

Abstract

Titanium dioxide (TiO_2) is a ubiquitous whitening compound widely used in topical products such as sunscreens, lotions and facial creams. The damaging health effects of TiO_2 inhalation has been widely studied in rats, mice and humans showing oxidative stress increase, DNA damage, cell death and inflammatory gene upregulation in lung and throat cells; however, the effects on skin cells from long-term topical use of various products remain largely unknown. In this study, we assessed the effect of specific TiO_2 nanoparticles (H_2TiO_7) on a human keratinocyte cell line (HaCaT). We performed a comparative analysis using three TiO_2 particles varying in size (Fine, Ultrafine and H_2TiO_7) and analyzed their effects on HaCaTs. There is a clear dose-dependent increase in superoxide production, caspase 8 and 9 activity, and apoptosis in HaCaTs after treatment with all three forms of TiO_2; however, there is no consistent effect on cell viability and proliferation with either of these TiO_2 particles. While there is data suggesting UV exposure can enhance the carcinogenic effects of TiO_2, we did not observe any significant effect of UV-C exposure combined with TiO_2 treatment on HaCaTs. Furthermore, TiO_2-treated cells showed minimal effects on VEGF upregulation and Wnt signaling pathway thereby showing no potential effect on angiogenesis and malignant transformation. Overall, we report here an increase in apoptosis, which may be caspase 8/Fas-dependent, and that the H_2TiO_7 nanoparticles, despite their smaller particle size, had no significant enhanced effect on HaCaT cells as compared to Fine and Ultrafine forms of TiO_2.

Keywords

Titanium dioxide, nanoparticles, apoptosis, keratinocytes, reactive oxygen species

History

Received 14 December 2015
Revised 7 March 2016
Accepted 28 April 2016
Published online 9 June 2016

Introduction

Titanium dioxide (TiO_2) is a globally produced oxide of titanium that is mined primarily from the naturally occurring minerals, rutile and anatase. It is primarily used as a pigment in several products ranging from paints, plastics and paper; to cosmetics, toothpastes and sunscreens due to its high refractive index, brightness and resistance to discoloration (Weir et al., 2012). During production, TiO_2 is processed into a wide range of particle sizes before incorporation into several products. While initial research has indicated that normal sized TiO_2 (>100 nm) has little to no effect on humans and animals; the demand for smaller sized TiO_2 nanoparticles (<100 nm), which can be used in a wider range of applications and products has increased rapidly since 2005 (Hendren et al., 2011; Hu et al., 2010; Iavicoli et al., 2011; Robichaud et al., 2009; Tucci et al., 2013).

Due to the ubiquitous usage of these TiO_2 nanoparticle-containing products, there is growing concern that the human population is at risk from over-exposure to TiO_2 and the health risks that come with this exposure. It is widely accepted that nanoparticles are more dangerous due to their increased effectiveness in invading the body facilitated by a larger surface area and more potent chemical reactivity (Lam et al., 2004). The dust from TiO_2 mining has been classified as an IARC Group 2B carcinogen by the International Agency for Research on Cancer (IARC) due to its ability to cause respiratory tract cancer in rats exposed to the powder (International Agency for Research on Cancer, 2010; Serpone & Kutal, 1993). There is also growing concern that the general population is at risk from direct usage of TiO_2-containing products and indirect exposure through food, garbage, water supply and of course by airborne means. While all forms and sizes of TiO_2 may be hazardous to human health, several studies have detailed the effects of nanoparticle inhalation that is primarily due to its small size. Inhaled nanoparticles have been found to cause an increase in oxidative stress; DNA damage; and the upregulation of pro-inflammatory and pro-apoptotic genes in human lung and endothelial cells (Agostini et al., 2011; Carinci et al., 2003; Manke et al., 2013; Peters et al., 2004). Inhaled nanoparticles are known to cross cell membranes infecting different areas of the body. They have been found in lung alveolar regions where they induce inflammation that triggers the development

Address for correspondence: Neelam Azad, Ph.D., Department of Pharmaceutical Sciences, Hampton University, Hampton, VA 23668, USA. Tel: +757 727 5071. Fax: +757 727 5840. E-mail: neelam.azad@hamptonu.edu

of granulomas; a precursor to pulmonary fibrosis and other forms of lung damage (Manke et al., 2013; Oberdorster et al., 2005; Shvedova & Kagan, 2010; Shvedova et al., 2005; Shvedova et al., 2008; Song et al., 2011; Turner-Warwick, 1963).

While the majority of the present research has explored the effects of nanoparticle inhalation on lung and respiratory tract tissue, there is still little understanding of the long-term effects of exposing skin cells to TiO_2 nanoparticle-containing products such as paper, rubber, ceramics, sunscreens, make-up and other cosmetic products. Several *in vivo* and *in vitro* studies have focused on the ability of different forms of TiO_2 to penetrate the dermal skin layer, and while the majority of research would indicate that this does not occur; there are data that indicate damaged skin can become susceptible to TiO_2 penetration (Miquel-Jeanjean et al., 2012; Schulz et al., 2002; Senzui et al., 2010; Tan et al., 1996). These results may vary based on the type of dermal damage and the overall characteristics of the skin. Exploring the TiO_2 nanoparticle dermal absorption theory is vital because skin exposure and contact is the most significant exposure route to TiO_2 nanoparticles for the general population (Tucci et al., 2013). The consensus is that once TiO_2 nanoparticles enter mammalian cells, through any route, it triggers a cellular reaction that includes an increase in oxidative stress; reduction in cell viability and proliferation; increase in cytokine production; and apoptosis: all potential precursors to malignancy, fibrosis and cancer.

The purpose of this study was to investigate the cytotoxic effects of TiO_2 nanoparticles (H_2TiO_7) on a human keratinocyte cell line and compare it to two other TiO_2 particles (Fine and Ultrafine). We analyzed the physiological and pathological processes that may be affected by TiO_2 exposure and by the size of the particles.

Materials and methods

Chemicals and reagents

Antibodies against Caspase 8 and 9, Bcl-2, Bid, pEGFR, EGFR, pAkt, Akt, β-Catenin, E-Cadherin, p53 and peroxidase-labeled secondary antibodies were obtained from Cell Signaling Technology (Danvers, MA). Antibodies for GAPDH and FLIP were obtained from Santa Cruz Biotechnologies (Dallas, TX), and the β-actin antibody was obtained from Sigma-Aldrich (St. Louis, MO). Mn (III) tetrakis (4-benzoic acid) porphyrin (MnTBAP) was obtained from Calbiochem (La Jolla, CA). Thiazolyl Blue Tetrazolium Bromide (MTT) and aminoguanidine (AG) were obtained from Sigma-Aldrich (St. Louis, MO). The oxidative probes, dichlorofluorescein diacetate (DCF-DA), 4,5-diaminofluorescein diacetate (DAF-DA) and dihydroethidium (DHE) were from Molecular Probes (Eugene, OR).

Cell culture

All cell lines were obtained from American Type Culture Collection (Manassas, VA). The immortalized human keratinocyte cell line (HaCaT) was cultured in Dulbecco's Modified Eagle medium (Thermo Scientific, Waltham, MA) supplemented with 10% fetal bovine serum (FBS), 2 mM L-glutamine, 100 U/mL penicillin and 100 mg/mL streptomycin. Human bronchial epithelial Beas-2B cells were cultured in Dulbecco's modified Eagle medium (Sigma-Aldrich) supplemented with 5% FBS, 2 mM L-glutamine, 100 U/mL penicillin and 100 μg/ml streptomycin. The human lung fibroblasts CRL-1490 were maintained in Eagle's Minimum Essential medium (MEM) supplemented with 10% FBS, 100 U/mL penicillin and 100 μg/mL streptomycin. All cell lines were grown in a 5% CO_2 environment at 37 °C.

Titanium dioxide characterization, preparation and cell treatment

TiO_2 particles H_2TiO_7, Fine (F) and Ultrafine (UF) were received as a gift from West Virginia University. The particle size of F-TiO_2 is 1 μm composed of 100% rutile (originally purchased from Sigma (#224227)). The particle size of UF-TiO_2 is 21 nm composed of 80% anatase and 20% rutile. The particle size of H_2TiO_7 is 12 nm and composed of 100% anatase. The stock solution of H_2TiO_7 nanoparticles (NP), Fine (F) and Ultrafine (UF) particles (2 mg/mL) was prepared by dissolving 10 mg of powder in 5 mL sterile PBS. This solution was then dispersed by sonicating (20% amplitude) for 90 s at 5 s intervals on ice to prevent aggregation and precipitation. The stock solutions were kept at 4 °C and used within 1–2 weeks for the experiments. Prior to each experiment, the stock solution was sonicated on ice as mentioned above and then immediately diluted into the working concentrations with medium. Titanium dioxide at different concentrations (0.1, 1, 10, 25 and 100 μg/cm^2) was calculated based on the surface area of the plate used (6-well, 12-well or 96-well plate). After treatments at various time points, plates were analyzed, or cells were harvested and prepared for protein analysis.

Reactive oxygen species/Reactive nitrogen species (ROS/RNS) detection

Cellular ROS/RNS production was determined fluorometrically using DHE, DCF-DA and DAF-DA as fluorescent probes for superoxide, peroxide and nitric oxide, respectively. After specific treatments, HaCaT cells were incubated with the probes (5 μM) for 30 min at 37 °C, after which they were washed, resuspended in PBS and analyzed for fluorescence intensity using All-In-One Microplate Reader (BioTek Instruments Inc.) at the excitation/emission wavelengths of 485/535 for DHE and 485/610 nm for DCF and DAF.

Caspase 8/9 assay

Caspase 8 and 9 activities were detected using the CaspGLOW™ Fluorescein Active Caspase-8 and -9 Staining Kit, respectively (BioVision, Milpitas, CA) according to the manufacturer's instructions. Briefly, HaCaT cells were seeded in 96-well plates at a concentration of 6.0×10^3 cells/well and treated with titanium dioxide for six hours. Cells were then trypsinized and 300 μL of each sample was placed in Eppendorf tubes. One microliter of FITC-LEHD-FMK was added to each tube and incubated for 30 min at 37 °C. Cells were then centrifuged at 3000 rpm for five minutes and the supernatant was removed. Samples were then resuspended in

Wash Buffer before being centrifuged as above. For analysis, samples were resuspended in 100 µL Wash Buffer and then plated on a black microtiter plate. Fluorescence intensity was measured at 485/535 nm. Wells containing unlabeled cells were used as control. The caspase inhibitor Z-VAD-FMK (1 µL/mL) was used as a negative control by pre-treating cells for one hour to inhibit caspase activation.

Western blotting

After specific treatments, HaCaT cells were incubated in lysis buffer containing 20 mM Tris–HCl (pH 7.5), 150 mM NaCl, 1 mM Na_2EDTA, 1 mM EGTA, 1% Triton, 2.5 mM sodium pyrophosphate, 1 mM β-glycerophosphate, 1 mM Na_3VO_4, and 1 µg/mL leupeptin (Cell Signaling), 100 mM PMSF, and a commercial protease inhibitor (Sigma-Aldrich) and phosphatase inhibitor (Pierce Biotechnology) mixture for 20 min on ice. After insoluble debris was precipitated by centrifugation at 10 000 rpm for 10 min at 4 °C, the supernatant was collected and assayed for protein content with bicinchoninic acid assay kit (Thermo Scientific). Equal amount of proteins per sample (20 µg) were resolved on 10% SDS-PAGE and transferred onto 0.45-mm nitrocellulose membranes. The transferred membranes were incubated overnight at 4 °C with appropriate primary antibodies diluted in 5% nonfat dry milk in Tris-buffered saline and Tween (25 mM Tris–HCl [pH 7.4], 125 mM NaCl, 0.05% Tween-20), followed by horseradish peroxidase-conjugated isotype-specific secondary antibodies for one hour at room temperature. The immune complexes were detected by chemiluminescence (Supersignal West Pico; Pierce Biotechnology, Rockford, IL) using a MyECL Imager (Thermo Scientific), and quantified by imaging densitometry using ImageJ (NIH, Image analysis using Java) digitizing software. Mean densitometry data from independent experiments were normalized to the control.

Apoptosis assay

Apoptosis was determined by Hoechst 33342 DNA fragmentation assay. Briefly, HaCaT cells were incubated with 10 µg/mL Hoechst 33342 nuclear stain (Life Technologies, Carlsbad, CA) for 30 min at 37 °C, and apoptosis determined by scoring the percentage of cells having intensely condensed chromatin and/or fragmented nuclei by fluorescence microscopy (EVOS All-in-one digital inverted fluorescence microscope) with software. From random fields 1000 nuclei were analyzed for each sample. The apoptotic index was calculated as apoptotic nuclei/total nuclei × 100 (%) using ImageJ software (Java image processing, NIH).

UV radiation

Plated HaCaT cells were exposed to UV-C irradiation from a 254 nm UV-C GE light bulb under a Labgard Class II Type A2 Biological safety cabinet (hood). Culture plates were irradiated with ~4, 8 and 40 J/m^2 for the 30 min, 1 h and 5 h time points accordingly.

MTT assay (cellular viability)

The MTT (3-(4,5-dimethylthiazol-2-yl)-2,5-diphenyltetrazolium bromide) colorimetric assay was performed in 96-well plates. Briefly, HaCaT cells were seeded in 96-well plates at a concentration of 6.0×10^3 cells/well and treated with titanium dioxide for 24 h. Twenty microliter of MTT solution (5 mg/mL) was then added to each well for three hours at 37 °C. The MTT solution was discarded and 100 µL dimethyl sulphoxide (DMSO) was added for 30 min while shaking to dissolve insoluble formazan crystal. Absorbance was measured at 570 nm. *Cell proliferation assay* – HaCaT, Beas-2B and CRL-1490 cells were plated in 96-well plates at a density of 1×10^3 cells/well in growth medium and were incubated for various time points (24 and 48 h). After specific treatments, the incubating medium was replaced with 50 µL of 1× CyQUANT™ dye-binding solution (Invitrogen) and incubated for 60 min at 37 °C. The fluorescence intensity of each sample was measured at the excitation and emission wavelengths of 485 and 535 nm, respectively.

Enzyme-linked immunosorbent assay (ELISA)

HaCaT cells were plated in a six-well plate at a density of 2×10^5 cells/well in culture medium and incubated overnight before the cells were subjected to treatment. After the treatment, cell supernatants were collected and analyzed for VEGF protein levels using a Human VEGFA ELISA kit (Thermo Scientific) per the manufacturer's protocol. Briefly, cell samples or reference standards (50 µL) were added to the wells of a microplate that was pre-coated with a monoclonal antibody specific to VEGF and incubated for 2 h at room temperature. After washing away unbounded substances, an HRP-conjugated polyclonal antibody against VEGF was added to the wells and incubated for 2 h at room temperature. After washing and adding 100 µL of substrate solution, optical density was determined on a microplate reader at 450 nm.

Collagen assay

Cellular collagen content was determined by Sircol® assay (Biocolor Ltd., Belfast, UK), according to the manufacturers' protocol. Briefly, Sirius red reagent (50 µL) was added to Beas-2B and CRL-1490 cell culture supernatants (50 µL) and mixed for 30 min. The collagen–dye complex was precipitated by centrifugation at 13 000 *g* for 5 min, washed with ethanol and dissolved in 0.5 M NaOH. The samples were read for absorbance at 540 nm.

Statistical analysis

The data represent means (±S.E.M.) from three or more independent experiments. Statistical analysis was performed by Student's *t* test at a significance level of $p < 0.05$.

Results

Effects of Fine (F), Ultrafine (UF) and H_2TiO_7 on cellular oxidative and nitrosative stress

The effects of F-TiO_2, UF-TiO_2 and H_2TiO_7 on cellular superoxide ($\cdot O_2^-$), hydrogen peroxide (H_2O_2) and nitric oxide (NO) levels were analyzed using specific fluorescent probes at three different time points. Figure 1(A) indicates that at the 15 min time-point there is a dose-dependent increase in hydrogen peroxide and superoxide levels over control for all three forms of TiO_2. However, there is no significant increase

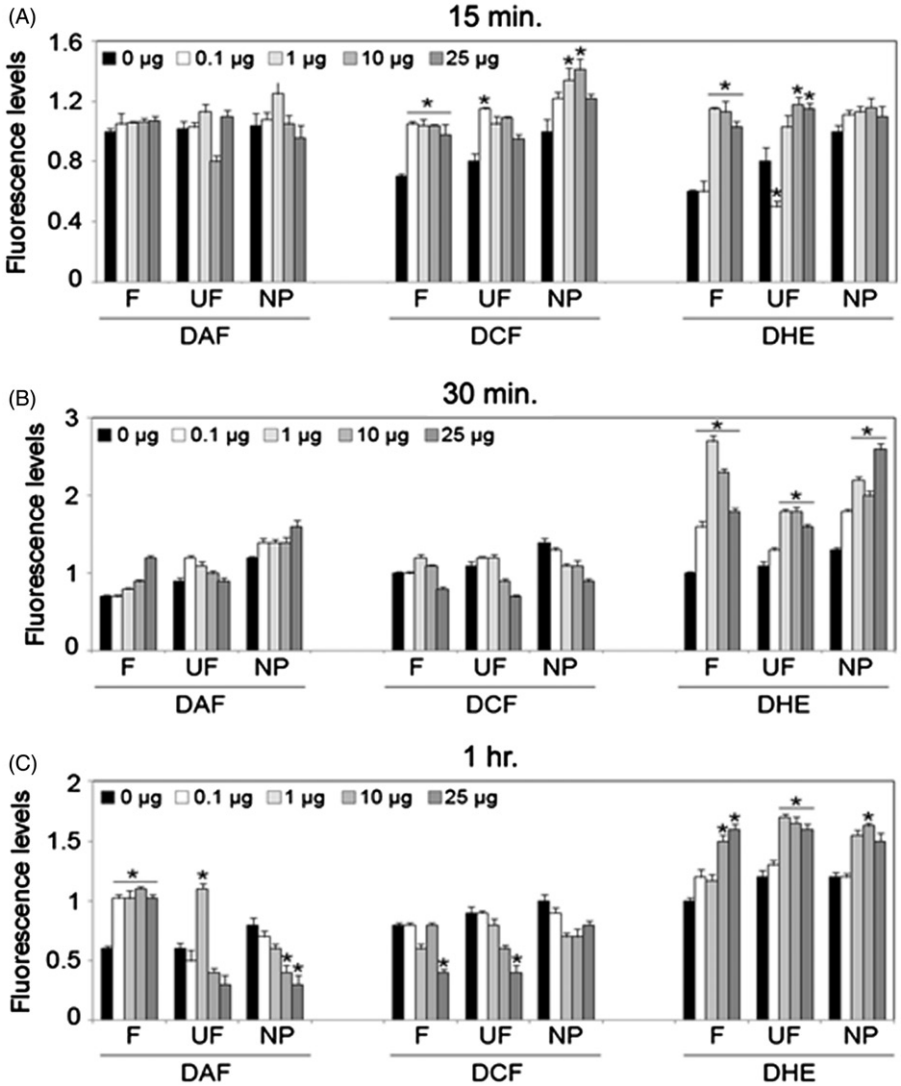

Figure 1. Effects of F-TiO_2, UF-TiO_2 and H_2TiO_7 on cellular oxidative stress. Subconfluent (90%) monolayers of HaCaT cells were treated with varying doses (0.1, 1, 10 and 25 µg) of F-TiO_2 (F), UF-TiO_2 (UF) and H_2TiO_7 (NP) for (A) 15 min, (B) 30 min and (C) 1 h. ROS/RNS levels were analyzed by spectrofluorometric measurement of DAF, DCF and DHE fluorescence for NO, hydrogen peroxide and superoxide, respectively. Graphs represent relative fluorescence intensity over untreated control. Data are mean ± S.E.M. ($n = 3$). *$p < 0.05$.

in NO levels for either form of TiO_2. In addition, no significant differences were observed in the effects elicited by F, UF and H_2TiO_7 on the skin cells. Figure 1(B and C) indicates a dose-dependent increase in superoxide levels at both the 30 min and one hour time points by all three forms of TiO_2 whereas there was a gradual decrease in hydrogen peroxide and NO levels. No significant differences were observed in the effects of F-TiO_2 and UF-TiO_2 versus H_2TiO_7.

Effects of F-TiO_2, UF-TiO_2 and H_2TiO_7 on apoptosis regulatory proteins

ROS accumulation in response to an external cell stressor can be followed by the activation of apoptotic cell death pathways (extrinsic or intrinsic). These pathways typically culminate with the activation of initiator caspases (caspase 8 and 9) that in turn activate additional caspases downstream which function in cell death. To determine if the upregulation of superoxide that we observe is triggering caspase activity toward apoptosis, HaCaT cells were treated with TiO_2 along with Z-VAD-FMK, a pan-caspase inhibitor. Caspase activity assay results indicate that at six hours there is a significant increase in caspase 8 activity as compared to control for all TiO_2 forms (Figure 2A). The increase in caspase 8 activity is ablated with Z-VAD-FMK pretreatment, verifying the effect of F-TiO_2, UF-TiO_2 and H_2TiO_7 on caspase 8. However, there is no delineation between the effect seen with F-TiO_2, UF-TiO_2 and H_2TiO_7 or the four doses administered. Figure 2(B) indicates that there were increases seen in active caspase 9 after TiO_2 treatment; however, the differences were much smaller as compared to caspase 8 activity levels (two-folds lower). Interestingly, caspase 9 activity was ablated when cells were treated with the higher dose of TiO_2 (25 µg/cm^2) for all three forms of TiO_2. Furthermore, the effect of TiO_2 on caspase 8 and 9 protein levels was analyzed by Western blotting. Figure 2(C) shows that at 24 h there are no changes in the cleavage and activation of caspase 8 or 9 for either form of TiO_2 as compared to control. The effect of all three TiO_2 particles was also assessed on other apoptosis regulatory proteins including FLIP, Bid and Bcl-2. Downregulation of the anti-apoptotic protein Bcl-2 by all three TiO_2 particles specifically at the treatment doses of 1 and 10 µg/cm^2 was observed. Treatment with TiO_2 particles also led to the downregulation of the pro-apoptotic protein Bid and had minimal effects on the expression of the anti-apoptotic protein, FLIP.

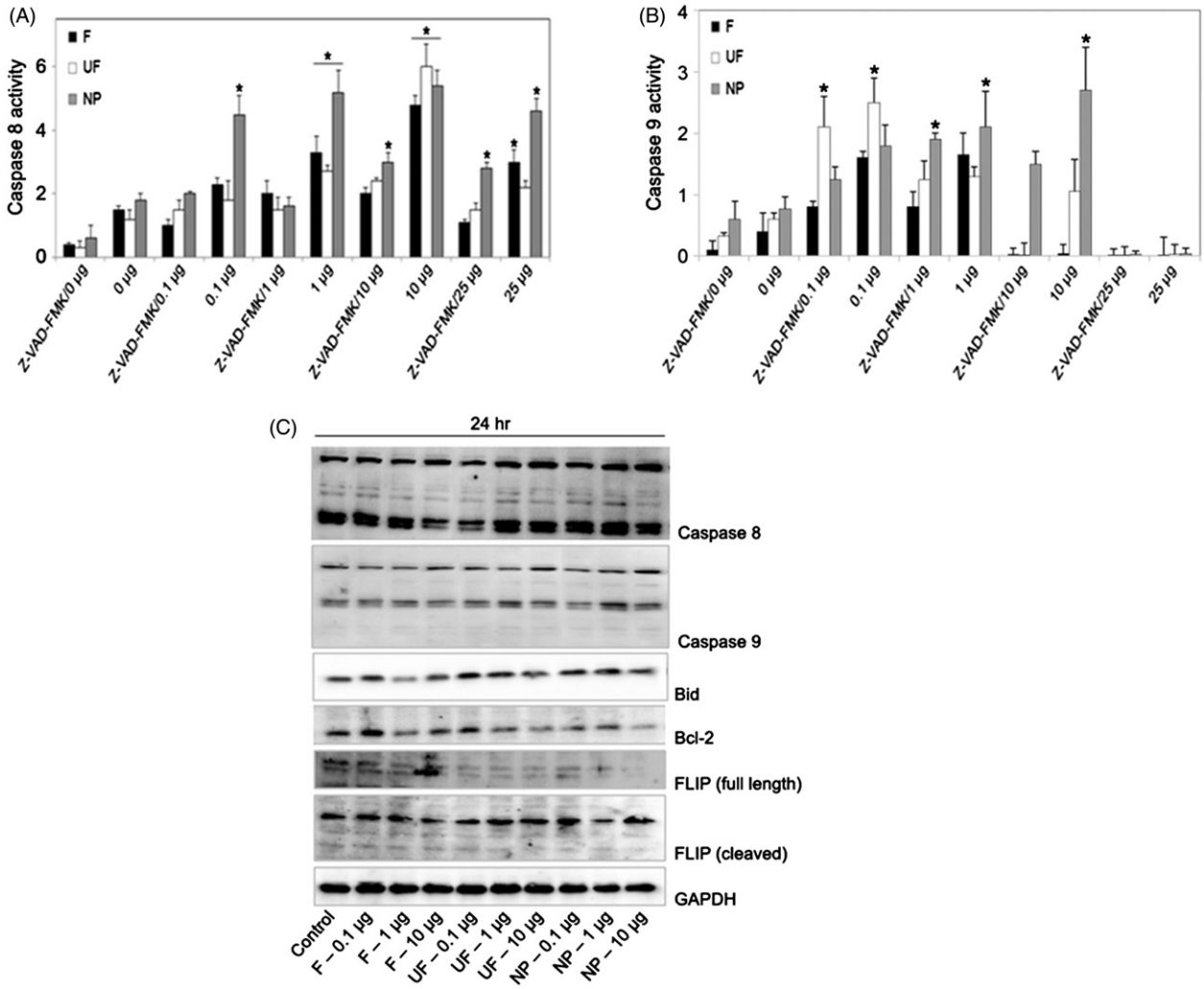

Figure 2. Effects of F-TiO_2, UF-TiO_2 and H_2TiO_7 on caspase activation and apoptosis. Subconfluent (90%) monolayers of HaCaT cells were either left untreated or pretreated with zVAD-FMK (10 µM) for 1 h followed by treatment with varying doses (0.1, 1, 10 and 25 µg/cm^2) of F-TiO_2 (F), UF-TiO_2 (UF) and H_2TiO_7 (NP) for 6 h and analyzed for (A) caspase 8 and (B) caspase 9 activity using specific fluorescent substrates IETD-AMC and LEHD-AMC, respectively. (C) Subconfluent (90%) monolayers of HaCaT cells were treated with varying doses (0.1, 1 and 10 µg/cm^2) of F-TiO_2 (F), UF-TiO_2 (UF) and H_2TiO_7 (NP) for 24 h before cell lysates were acquired and analyzed for apoptotic-related protein expression by Western blotting. GAPDH was used as a loading control.

Effects of F-TiO_2, UF-TiO_2 and H_2TiO_7 on apoptosis

To determine if the TiO_2-induced superoxide accumulation and increase in caspase activity that we observed in HaCaTs leads to cell death, we next analyzed apoptosis. We characterized the apoptotic response of HaCaT cells treated with varying concentrations (0.1–25 µg) of all three forms of TiO_2. Apoptosis was analyzed after 12 h and 24 h by Hoechst 33342 assay. TiO_2 treatment caused a significant increase in apoptosis versus control at both the 12 and 24-h time points (Figure 3(A and B)). There were no clear differences in the effect on cell death between F-TiO_2, UF-TiO_2 and H_2TiO_7. However there was a significant reduction in cell death at both time points when cells were treated with the dose of 25 µg of F-TiO_2, UF-TiO_2 and H_2TiO_7 indicating that 25 µg might be a saturated dose that has only minor effects on HaCaT cells. We further analyzed the effects of ROS and NO modulators on TiO_2-induced apoptosis. HaCaT cells were pretreated with either Aminoguanidine (AG), a nitric oxide synthase (NOS) inhibitor, or the superoxide dismutase (SOD) mimetic and peroxynitrite scavenger, MnTBAP, followed by treatment with -TiO_2, UF-TiO_2 and H_2TiO_7 for 24 h. Figure 3(C) shows an increase in cell death over control for all three forms and all doses of TiO_2. However, pretreatment with either AG or MnTBAP had no significant effect on TiO_2-induced apoptosis. We next assessed the combined effect of short-wavelength ultraviolet (UV-C) rays pre-exposure and TiO_2 treatment on apoptosis. Numerous published reports have indicated that UV exposure (UV-A, UV-B, UV-C) can enhance apoptosis by increasing DNA damage. To determine if UV exposure exacerbates the effect of various TiO_2 particles on cell death, HaCaTs were exposed to UV-C rays for three different time points (~4, 8 and 40 J/m^2) prior to treatment with three different doses of F-TiO_2, UF-TiO_2 and H_2TiO_7. Figure 3(D) shows no difference in the percentage of cell death observed after TiO_2 treatment with pre-exposure to UV-C at the various time points (0.5, 1 and 5 h) in comparison to the cell death observed after TiO_2 treatment alone (Figure 3(A and B)).

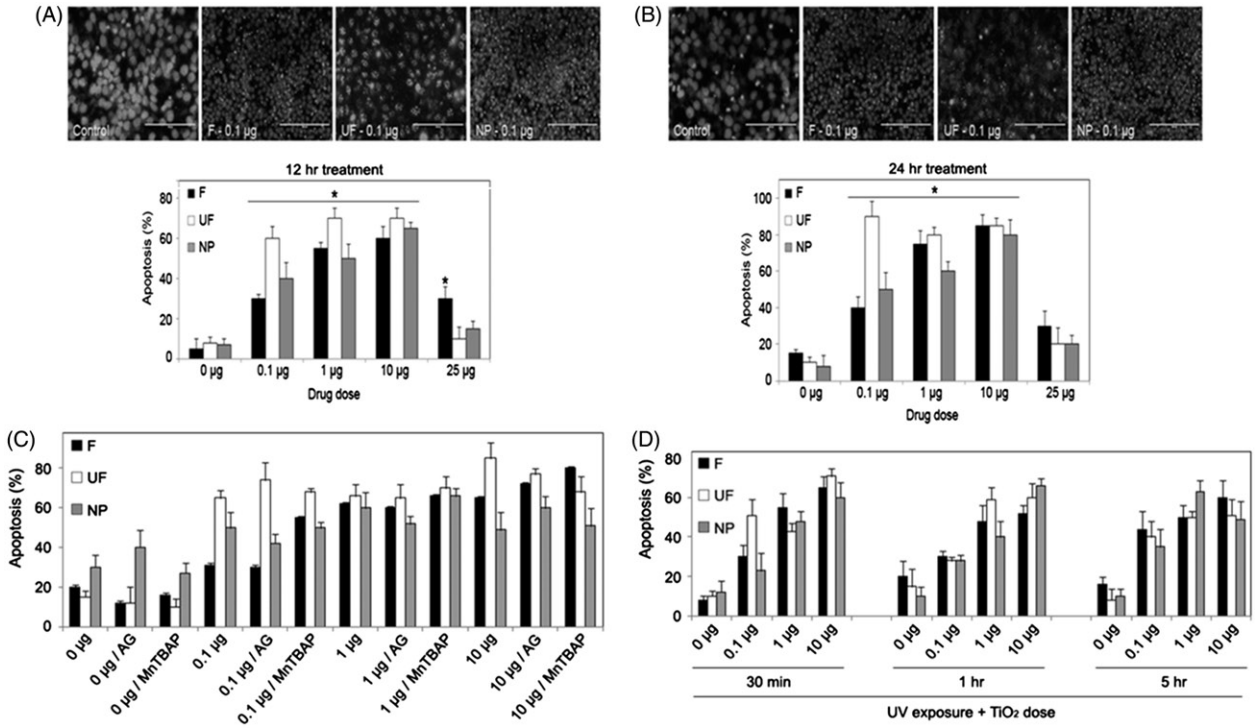

Figure 3. Effects of ROS modulators and UV-C pretreatments on TiO_2-induced cell death. Subconfluent (90%) monolayers of HaCaT cells were treated with varying doses (0.1, 1, 10 and 25 µg/cm^2) of F-TiO_2 (F), UF-TiO_2 (UF) and H_2TiO_7 (NP) for (A) 12 h and (B) 24 h and analyzed for apoptosis by Hoechst 33342 assay. Representative fluorescence micrographs of treated cells stained with the Hoechst dye are shown. Apoptotic cells exhibited shrunken and fragmented nuclei with bright nuclear fluorescence. (C) Subconfluent (90%) monolayers of HaCaT cells were either left untreated or pretreated with AG (300 µM) or MnTBAP (100 µM) for 1 h followed by treatment with varying doses (0.1, 1 and 10 µg/cm^2) of F-TiO_2 (F), UF-TiO_2 (UF) and H_2TiO_7 (NP) for 24 h and analyzed for apoptosis by Hoechst 33342 assay. (D) Cells were seeded as above and exposed to UV-C light (~4, 8 and 40 J/m^2) for three different time points (30 min, 1 h and 5 h) followed by treatment with varying doses (0.1, 1 and 10 µg/cm^2) of F-TiO_2 (F), UF-TiO_2 (UF) and H_2TiO_7 (NP) for 24 h and analyzed for apoptosis as above. Data are mean ± S.E.M. ($n = 3$). *$p < 0.05$.

Effects of F-TiO_2, UF-TiO_2 and H_2TiO_7 on cell proliferation and angiogenesis

To determine if TiO_2 has carcinogenic potential when exposed to keratinocytes, we analyzed the effect of TiO_2 particles on cell viability and proliferation using MTT and CyQUANT assays, respectively. Figure 4(A) demonstrates that F-TiO_2 and UF-TiO_2 had positive effects on cell viability at 24 h, while the opposite effect was observed when cells were treated with H_2TiO_7. Furthermore, cell proliferation was negatively affected in response to all treatment doses of F-TiO_2, UF-TiO_2 and H_2TiO_7 at the 48-h time-point, with the 25 µg/cm^2 dose of H_2TiO_7 having the most pronounced effect (Figure 4B). To assess the effect of TiO_2 on angiogenesis in keratinocytes, we analyzed the central angiogenic mediator, vascular endothelial growth factor (VEGF) levels. Figure 4(C) demonstrates that there was no significant change in cellular VEGF levels in cells treated with various doses of all three TiO_2 particles at the 24-h time point.

Effects of F-TiO_2, UF-TiO_2 and H_2TiO_7 on cell survival and differentiation pathways

The effect of F-TiO_2, UF-TiO_2 and H_2TiO_7 was analyzed on epidermal growth factor receptor (EGFR), a known stimulator of cell growth when activated by phosphorylation, and Akt, a serine/threonine protein kinase that functions in several cellular processes including cell death and proliferation. At the six-hour time point, TiO_2 particles had a minimal effect on phosphorylated EGFR levels, while Akt phosphorylation and hence activation increased specifically with 10 µg/cm^2 UF-TiO_2 and 1 µg/cm^2 H_2TiO_7 doses (Figure 5A). HaCaT cells were then treated with varying concentrations of UF-TiO_2 and H_2TiO_7 for 12 and 24 h, and probed for differentiation marker proteins including E-Cadherin and β-Catenin. Figure 5(B) demonstrates that there is minimal effect of UF-TiO_2 and H_2TiO_7 treatments on the expression of these proteins. E-Cadherin protein expression is downregulated at 12 h and β-Catenin is downregulated at 24 h as compared to control in response to both H_2TiO_7 and UF-TiO_2 treatments. At both 12 and 24-h time-points, p53 expression remains unchanged in all conditions.

Effects of F-TiO_2, UF-TiO_2 and H_2TiO_7 on human lung epithelial and fibroblast cell proliferation

Since the majority of TiO_2 nanoparticle research both *in vitro* and *in vivo* has focused on the effect of these particles on lung and throat tissue, we analyzed the effects of the three forms of TiO_2 on lung cells. Beas-2B (human lung epithelial) cells and CRL-1490 (lung fibroblast) cells were treated with varying doses of F-TiO_2, UF-TiO_2 and H_2TiO_7. All TiO_2 particles showed an inhibitory effect on Beas-2B cell proliferation at both the 24 h and 48 h time-points (Figure 6A). Figure 6(B) shows a moderate increase in cell proliferation in CRL-1490 cells. To further determine the potential of TiO_2 to induce proliferation and invasion in these two cell lines, we analyzed collagen levels using Sircol® assay after treatment for 24 h with varying doses of TiO_2. Figure 6(C) shows fluctuating

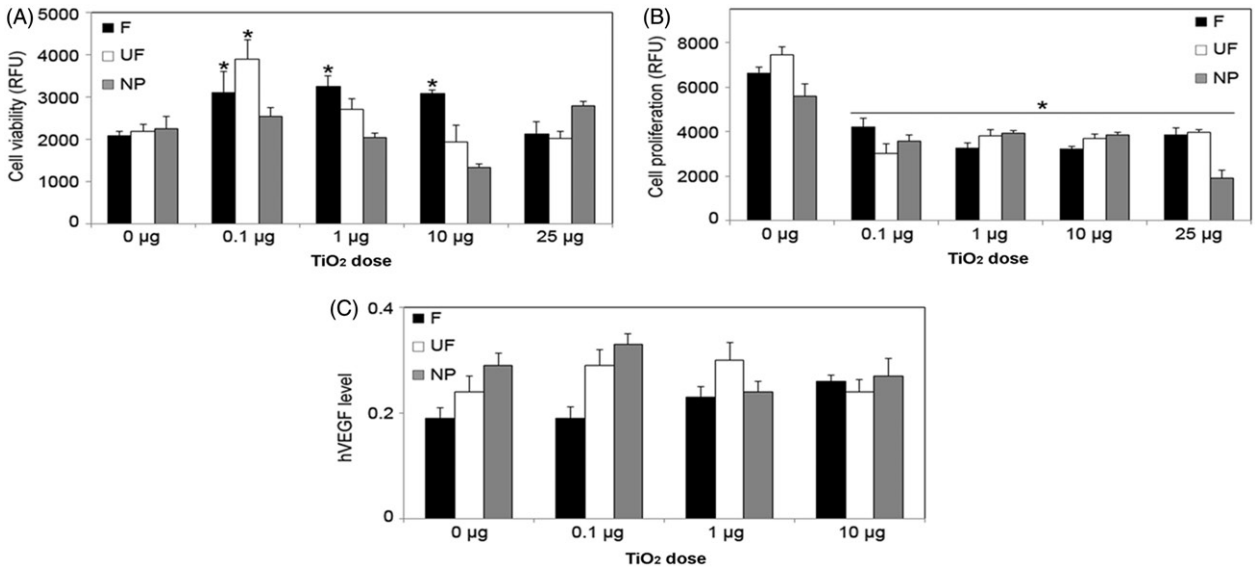

Figure 4. Effects of F-TiO_2, UF-TiO_2, and H_2TiO_7 on cell viability, proliferation, and VEGF levels. (A) Subconfluent (90%) monolayers of HaCaT cells were treated with varying doses (0.1, 1, 10 and 25 µg/cm^2) of F-TiO_2 (F), UF-TiO_2 (UF) and H_2TiO_7 (NP) for 24 h and analyzed for cell viability using MTT assay. (B) HaCaT cells were treated as above and analyzed after 48 h for cell proliferation using CyQUANT® dye reagent. (C) HaCaT cells were treated with varying doses (0.1, 1 and 10 µg/cm^2) of F-TiO_2 (F), UF-TiO_2 (UF) and H_2TiO_7 (NP) for 24 h and analyzed for VEGF levels by ELISA. Data are mean ± S.E.M. ($n = 3$). *$p < 0.05$.

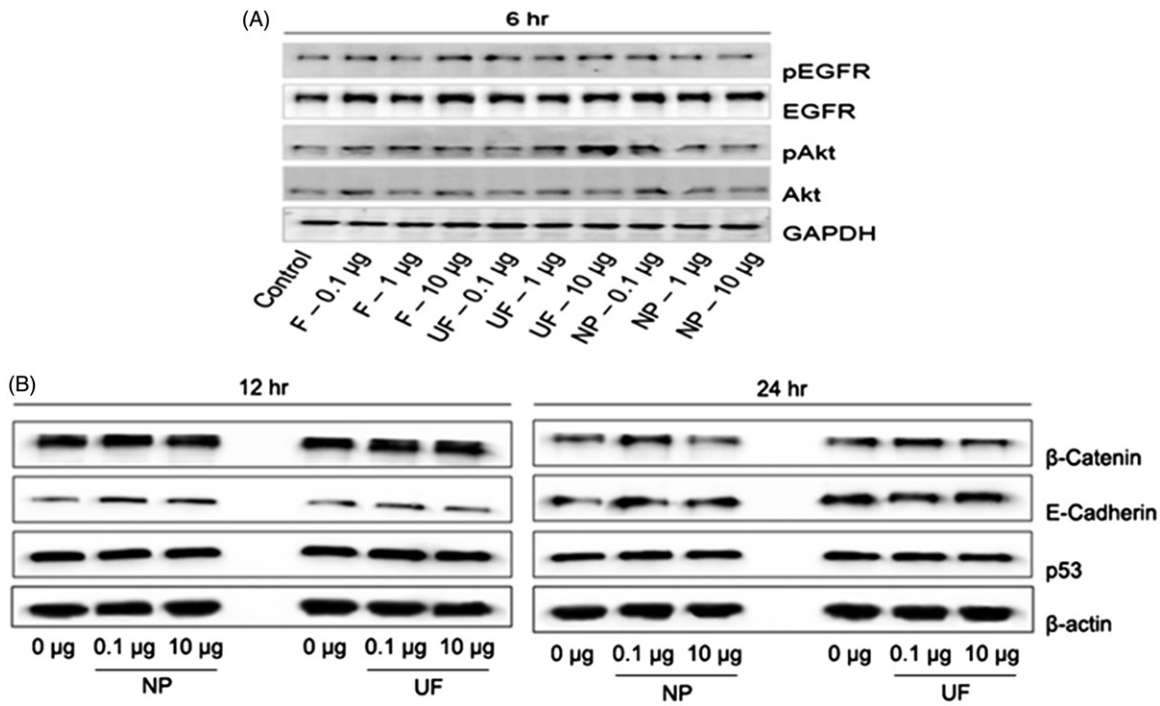

Figure 5. Effects of F-TiO_2, UF-TiO_2 and H_2TiO_7 on cell survival and EMT proteins. (A) Subconfluent (90%) monolayers of HaCaT cells were treated with varying doses (0.1, 1 and 10 µg/cm^2) of F-TiO_2 (F), UF-TiO_2 (UF), and H_2TiO_7 (NP) for 6 h before cell lysates were acquired and analyzed for phosphorylated and total EGFR and Akt proteins. GAPDH was used as a loading control. (B) Cells were seeded as above and treated with two doses (0.1 and 10 µg/cm^2) of UF-TiO_2 (UF) and H_2TiO_7 (NP) for 12 h and 24 h and cell lysates were analyzed for β-Catenin, E-Cadherin and p53 proteins by Western blotting. β-Actin was used as a loading control.

changes in collagen levels as compared to control in both cell lines at various doses and with the different forms of TiO_2. The most pronounced reduction in collagen levels was observed with the lowest (0.1 µg/cm^2) and highest (100 µg/cm^2) doses of each F-TiO_2, UF-TiO_2 and H_2TiO_7. This data correlated with cell proliferation results for Beas-2B cells but not for CRL-1490 cells. TiO_2 particles inhibited Beas-2B cell proliferation and endogenous collagen levels, whereas the effect on CRL-1490 cells is not conclusive.

Discussion

Due to the widespread use of TiO_2 nanoparticles in several products including cosmetics and other topical products, it is

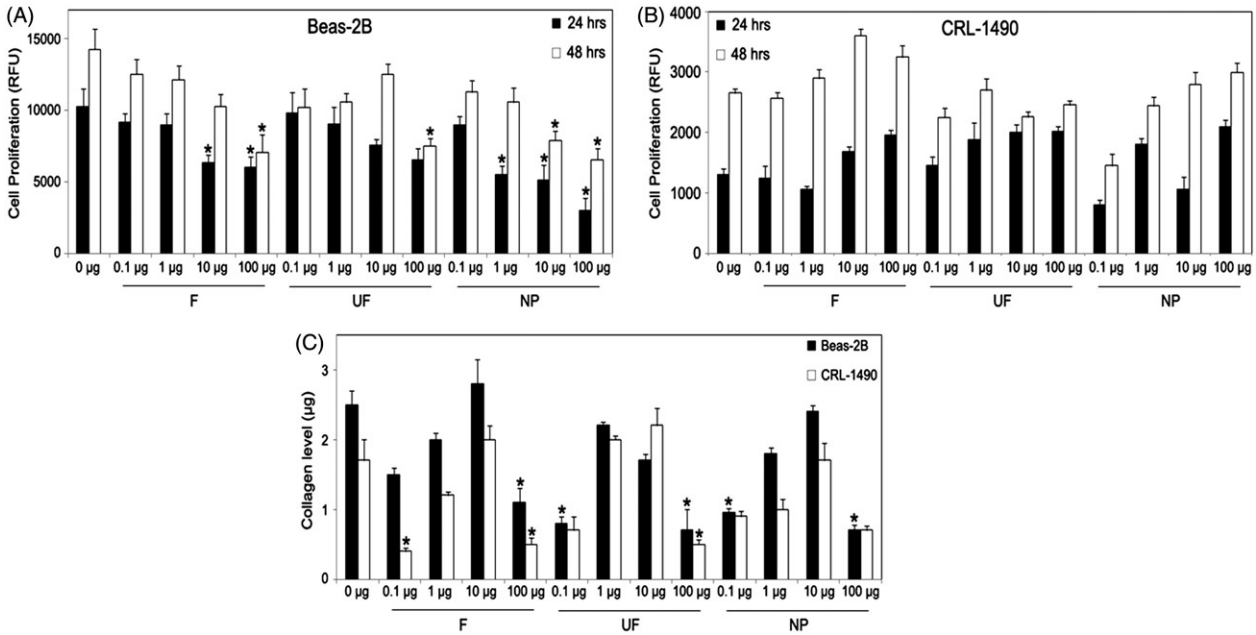

Figure 6. Effects of F-TiO_2, UF-TiO_2 and H_2TiO_7 on human lung epithelial and fibroblast cells. Subconfluent (90%) monolayers of (A) Beas-2B and (B) CRL-1490 cells were treated with varying doses (0.1, 1, 10 and 100 µg/cm^2) of UF-TiO_2 (UF) and H_2TiO_7 (NP) for 24 h and 48 h and analyzed for cell proliferation using the CyQUANT® dye reagent. (C) Beas-2B and CRL-1490 cells were seeded as above and treated with varying doses (0.1, 1, 10 and 100 µg/cm^2) of UF-TiO_2 (UF) and H_2TiO_7 (NP) for 24 h and analyzed for collagen levels using the Sircol® collagen assay kit. Data are mean ± S.E.M. ($n = 3$). *$p < 0.05$.

important to understand the potential cytotoxic effects of TiO_2 due to long-term use of these products. While TiO_2 has been shown to be a lung and throat carcinogen when inhaled and/or swallowed through TiO_2 mining or product use, the long-term effects of physical contact with the dermis through topical product usage is understudied. Even though the majority of research articles report no skin penetration by TiO_2 nanoparticles, there is still evidence that damaged dermal layers can facilitate TiO_2 absorption, and absorption rates and levels vary based on the age and quality of the dermis layer that is exposed to TiO_2 nanoparticles. Because direct skin contact is the most common risk factor for TiO_2 nanoparticles exposure to the human population, it is pertinent that we fully understand the long-term effects of exposure to TiO_2.

The skin is the largest organ in the body and provides protection through two layers: the epidermis and dermis. It serves as the first line of defense against topically applied substances, and functions in the metabolism of any external reagents that penetrate the skin (Tucci et al., 2013). There are several cancer pathologies that originate through the skin layers that include melanoma, carcinogenesis and dermatitis, which is initiated by cytokine release and dermal cell inflammation facilitated by an increase in ROS generation. Several *in vitro* studies have reported oxidative stress induction and cell death in mammalian cells treated with TiO_2 nanoparticles. In this study, we analyzed the effects of F-TiO_2, UF-TiO_2 and H_2TiO_7 on oxidative stress levels in human skin cells (keratinocytes). We observed a significant dose-response increase in superoxide levels for all three particles used at 15 and 30 min, as well as the 1 h time point (Figure 1). It is known that ROS induction can mediate and regulate caspase-related cell death pathways, specifically Fas-mediated apoptotic cell death that proceeds through the FADD complex pathway by way of caspase 8 activation (Izeradjene et al., 2005; Thornberry & Lazebnik, 1998; Yoo et al., 2012). Specifically, an increase in superoxide production has been repeatedly shown to be a precursor to TiO_2-induced cell death in various cell lines (Masoud et al., 2015; Niska et al., 2015). It is feasible that the reason ROS scavengers used in Figure 3 had no effect on TiO_2-induced apoptosis in HaCaTs is because of the difference in time points used to analyze apoptosis in Figure 3 (12 and 24 h) versus ROS production in Figure 1 (15 and 30 min, 1 h). The data clearly shows that superoxide levels increase rapidly immediately following TiO_2 treatment, which may be the required early precursor to the cell death we observe at the later time points.

Caspase data indicated that TiO_2 treatment significantly activated caspase 8, and to a lesser extent caspase 9, as compared to control (Figure 2(A and B)). This was corroborated by utilizing a pan-caspase inhibitor, Z-VAD-FMK, which attenuated the caspase 8 activation observed with TiO_2 treatment. H_2TiO_7-mediated activation of caspase 8, indicates that the cell death observed in HaCaT cells may be induced by Fas as previously reported (Yoo et al., 2012). While an increase in oxidative stress is consistently shown in TiO_2-related studies as mentioned above, the absence of this ubiquitous effect in our system was further corroborated by using NOS (AG) and SOD mimetic/peroxynitrite inhibitor (MnTBAP). Both inhibitors had no significant effect on HaCaT cell death observed in response to TiO_2 treatment (Figure 3) suggesting that TiO_2-induced apoptosis in HaCaT cells is not solely dependent on oxidative stress.

The various TiO_2 particles significantly induced apoptosis in HaCaT cells (Figure 3) but there was minimal

activation and involvement of various apoptosis-related proteins including FLIP, Bid and Bcl-2 at the 24-h time-point (Figure 2). Analysis of the tumor suppressor and apoptotic initiator p53 indicated no change in expression over control (Figure 5). Furthermore, there was no delineation between F-TiO_2, UF-TiO_2 and H_2TiO_7, thereby indicating that particle size played no significant role in the apoptosis inducting effects of TiO_2. The FLIP protein is known to interact with pro-caspase 8 and the FADD complex in both a pro- and anti-apoptotic manner (Dohrman et al., 2005). Although FLIP protein was not affected, activation of caspase 8 indicated that TiO_2-induced cell death observed in HaCaT cells may be mediated through the Fas-FADD-apoptotic pathway. Ultraviolet (UV) rays can contribute to increased free radical production and accumulation thereby stimulating skin inflammation. It has been reported that pre-exposing cells to UV radiation can enhance the cytotoxicity effects of nanoparticles, specifically TiO_2 (Cai et al., 1992; Zhang & Sun, 2004). Kang et al. reported that in the presence of UVA, TiO_2 nanoparticle treatment caused a significant decrease in cell viability, increased ROS and induced activation of pro-apoptotic proteins such as caspase 9 and 3 in peripheral blood lymphocytes (Kang et al., 2011). However, our data indicates that UV-C exposure at the indicated time points had no significant effect on TiO_2-induced apoptosis in HaCaT cells (Figure 3(D)). It must be pointed out that UV-C rays are significantly weaker than the ozone-penetrating UV-A and UV-B rays humans are exposed to daily. Despite UV-C rays being weaker rays that emit less irradiation; there are several publications that utilize these rays in studies that result in significant ROS accumulation and apoptosis (Dunkern et al., 2001; Jiang et al., 2014). Future experimental analysis utilizing UV-A and UV-B radiation may unearth an additive effect with TiO_2 that enhances apoptosis or cell proliferation toward a malignant phenotype.

Cell proliferation, invasion, migration and angiogenesis are key characteristic features for malignant transformation and tumor development. TiO_2 particles had a clear negative effect on cell proliferation as compared to control. The major cellular regulator of angiogenesis, VEGF, which functions in vascular permeability and angiogenesis by inducing cell proliferation, migration and elongation, network formation and branching of endothelial cells (Azad et al., 2013; Carmeliet, 2000), was also analyzed. F-TiO_2, UF-TiO_2 and the H_2TiO_7 had no significant effect on cellular VEGF levels (Figure 4(C)). In addition, we observed changes in pAkt and pEGFR protein expression levels in TiO_2-treated cells (Figure 5). Akt and EGFR are both involved in apoptosis, cell proliferation, differentiation and migration; indicating a possible link with malignancy formation in TiO_2-treated skin cells. To investigate this further, we analyzed the possibility of TiO_2 having a metastatic effect on HaCaT cells precluded by cell migration and differentiation. The canonical Wnt signaling pathway functions in embryonic development by regulating gene transcription for cell proliferation, differentiation and specifically migration. The Wnt signaling pathway plays a key role in carcinogenesis and tumor development characterized by the upregulation or mutation of the β-Catenin gene; a mutation that is found in a wide variety of human cancers including melanoma, pancreatic and ovarian cancer (Anastas & Moon, 2013; Taketo, 2004). In conjunction with the Wnt signaling pathway, epithelial mesenchymal transition (EMT) is a process by which cells become invasive and migratory leading to metastasis that is initiated by the loss of E-Cadherin function/expression. β-Catenin dysregulation coupled with E-Cadherin down-regulation leads to the loss of cell-cell adhesion, invasion and migration; important cellular changes seen in several malignancies including fibrosis, breast cancer and melanoma (Chaffer & Weinberg, 2011; Singh & Settleman, 2010). Analysis of the expression of both of these critical proteins indicated minor changes in TiO_2-treated cells versus control with no overexpression of β-Catenin or downregulation of E-Cadherin (Figure 5). The expression pattern of both β-Catenin and E-Cadherin here indicates that F-TiO_2, UF-TiO_2 and H_2TiO_7 particles do not regulate Wnt signaling pathway or EMT, and therefore do not affect metastasis and malignancy in HaCaT cells.

TiO_2 is mined from minerals such as rutile and anatase. The dust released from this mining process has been classified as a Group 2B carcinogen by the IARC due to the possibility of it being carcinogenic to humans (International Agency for Research on Cancer, 2010). Recent evidence has shown that this TiO_2 dust can cause respiratory tract cancer in mice (Hu et al., 2010; Lam et al., 2004), and lung cell injury with mutation and fibrosis in humans who work in these dusty environments (Hendren et al., 2011; Robichaud et al., 2009). Several *in vivo* studies have also linked exposure to airborne nanoparticles with pulmonary fibrosis development due to inflammation and the formation of granulomas that migrate and invade lung tissue (Azad et al., 2013; Shvedova et al., 2005; Shvedova et al., 2008; Wang et al., 2010; Warheit et al., 2004). We analyzed the effects of F-TiO_2, UF-TiO_2 and H_2TiO_7 particles on two different types of lung cells (epithelial and fibroblast). We observed a decrease in collagen levels in both lung cell lines in response to TiO_2 treatment (Figure 6). This result suggests that short-term exposure of lung tissue to TiO_2 has no deleterious effects. The effect on cell proliferation was inhibitory in Beas-2B cells but was not conclusive for CRL-1490 lung cells. The effect of H_2TiO_7 was not different from F-TiO_2 or UF-TiO_2, confirming in different cell-lines that smaller particle size and increased surface area of H_2TiO_7 does not translate into more deleterious effects on various cellular properties.

Conclusions

In summary, F-TiO_2, UF-TiO_2 and H_2TiO_7 particles induce apoptosis in keratinocytes through caspase 8 and the Fas/FADD pathway. There is a dose-dependent increase in superoxide accumulation and caspase 8 and 9 activity; which are followed by a similar trend in apoptosis. However there was no significant difference in the effects of H_2TiO_7 nanoparticles as compared to F-TiO_2 and UF-TiO_2. We also report that the various TiO_2 particles had no consistent effects on cell proliferation, viability and angiogenic/migration/invasion potential in HaCaT keratinocytes and two different lung cell types (Beas-2B and CRL-1490). The increased

carcinogenic potential of H_2TiO_7 due to its increased surface area and smaller particle size, does not translate into more deleterious effects in skin and lung cells, as compared to the other forms of TiO_2. While this study does not focus on the long-term effects that exposure to TiO_2 may have on skin cells; the inconsistent and inconclusive results here corroborate previously published data on the effect of TiO_2 on skin cells. This data reaffirms the accepted conclusion that the effect of TiO_2 is dependent on the integrity of the epidermal skin layer (more effective on damaged tissue), and the genetic characteristics of the skin layer being exposed to the nanoparticles. Further analysis using long-term exposure studies is definitely needed to determine the cytotoxic or malignant potential of TiO_2 nanoparticles on human skin cells. This analysis will allow us to make conclusive determinations on what effect, if any, chronic exposure to TiO_2 is having on the human populous.

Declaration of interest

None of the authors has a financial relationship with a commercial entity that has an interest in the subject of this manuscript. The findings and conclusions in this report are those of the authors and do not necessarily represent the views of the National Institute for Occupational Safety and Health (NIOSH).

Contract grant sponsor: National Institutes of Health; Contract grant numbers: HL112630 and CA173069.

References

Agostini M, Tucci P, Melino G. (2011). Cell death pathology: perspective for human diseases. Biochem Biophys Res Commun 414:451–455.

Anastas JN, Moon RT. (2013). WNT signalling pathways as therapeutic targets in cancer. Nat Rev Cancer 13:11–26.

Azad N, Iyer AK, Wang L, et al. (2013). Reactive oxygen species-mediated p38 MAPK regulates carbon nanotube-induced fibrogenic and angiogenic responses. Nanotoxicology 7:157–168.

Cai R, Kubota Y, Shuin T, et al. (1992). Induction of cytotoxicity by photoexcited TiO_2 particles. Cancer Res 52:2346–2348.

Carinci F, Volinia S, Pezzetti F, et al. (2003). Titanium-cell interaction: analysis of gene expression profiling. J Biomed Mater Res B Appl Biomater 66:341–346.

Carmeliet P. (2000). Mechanisms of angiogenesis and arteriogenesis. Nat Med 6:389–395.

Chaffer CL, Weinberg RA. (2011). A perspective on cancer cell metastasis. Science 331:1559–1564.

Dohrman A, Kataoka T, Cuenin S, et al. (2005). Cellular FLIP (long form) regulates CD8+ T cell activation through caspase-8-dependent NF-kappa B activation. J Immunol 174:5270–5278.

Dunkern TR, Fritz G, Kaina B. (2001). Ultraviolet light-induced DNA damage triggers apoptosis in nucleotide excision repair-deficient cells via Bcl-2 decline and caspase-3/-8 activation. Oncogene 20: 6026–6038.

Hendren CO, Mesnard X, Droge J, Wiesner MR. (2011). Estimating production data for five engineered nanomaterials as a basis for exposure assessment. Environ Sci Technol 45:2562–2569.

Hu R, Gong X, Duan Y, et al. (2010). Neurotoxicological effects and the impairment of spatial recognition memory in mice caused by exposure to TiO_2 nanoparticles. Biomaterials 31:8043–8050.

Iavicoli I, Leso V, Fontana L, Bergamaschi A. (2011). Toxicological effects of titanium dioxide nanoparticles: a review of in vitro mammalian studies. Eur Rev Med Pharmacol Sci 15:481–508.

International Agency for Research on Cancer. (2010). IARC monographs on the evaluation of carcinogenic risks to humans. Vol. 93: carbon black, titanium dioxide, and talc. Lyon, France: IARC, 1-413.

Izeradjene K, Douglas L, Tillman DM, et al. (2005). Reactive oxygen species regulate caspase activation in tumor necrosis factor-related apoptosis-inducing ligand-resistant human colon carcinoma cell lines. Cancer Res 65:7436–7445.

Jiang Y, Ge XY, Liu SM, et al. (2014). Nimotuzumab suppresses epithelial-mesenchymal transition and enhances apoptosis in low-dose UV-C treated salivary adenoid cystic carcinoma cell lines in vitro. Anticancer Drugs 25:1052–1060.

Kang SJ, Lee YJ, Kim BM, et al. (2011). Cytotoxicity and genotoxicity of titanium dioxide nanoparticles in UVA-irradiated normal peripheral blood lymphocytes. Drug Chem Toxicol 34:277–284.

Lam CW, James JT, McCluskey R, Hunter RL. (2004). Pulmonary toxicity of single-wall carbon nanotubes in mice 7 and 90 days after intratracheal instillation. Toxicol Sci 77:126–134.

Manke A, Wang L, Rojanasakul Y. (2013). Mechanisms of nanoparticle-induced oxidative stress and toxicity. Biomed Res Int 2013:942916.

Masoud R, Bizouarn T, Trepout S, et al. (2015). Titanium dioxide nanoparticles increase superoxide anion production by acting on NADPH oxidase. PLoS One 10:e0144829.

Miquel-Jeanjean C, Crepel F, Raufast V, et al. (2012). Penetration study of formulated nanosized titanium dioxide in models of damaged and sun-irradiated skins. Photochem Photobiol 88:1513–1521.

Niska K, Pyszka K, Tukaj C, et al. (2015). Titanium dioxide nanoparticles enhance production of superoxide anion and alter the antioxidant system in human osteoblast cells. Int J Nanomed 10: 1095–1107.

Oberdorster G, Oberdorster E, Oberdorster J. (2005). Nanotoxicology: an emerging discipline evolving from studies of ultrafine particles. Environ Health Perspect 113:823–839.

Peters K, Unger RE, Kirkpatrick CJ, et al. (2004). Effects of nano-scaled particles on endothelial cell function in vitro: studies on viability, proliferation and inflammation. J Mater Sci Mater Med 15: 321–325.

Robichaud CO, Uyar AE, Darby MR, et al. (2009). Estimates of upper bounds and trends in nano-TiO_2 production as a basis for exposure assessment. Environ Sci Technol 43:4227–4233.

Schulz J, Hohenberg H, Pflucker F, et al. (2002). Distribution of sunscreens on skin. Adv Drug Deliv Rev 54:S157–S163.

Senzui M, Tamura T, Miura K, et al. (2010). Study on penetration of titanium dioxide (TiO(2)) nanoparticles into intact and damaged skin in vitro. J Toxicol Sci 35:107–113.

Serpone N, Kutal C, eds. (1993). Photosensitive metal-organic systems: mechanistic principles and applications. Advances in Chemistry series. Vol. 238. Washington DC: ACS, 450.

Shvedova AA, Kagan VE. (2010). The role of nanotoxicology in realizing the 'helping without harm' paradigm of nanomedicine: lessons from studies of pulmonary effects of single-walled carbon nanotubes. J Intern Med 267:106–118.

Shvedova AA, Kisin E, Murray AR, et al. (2008). Inhalation vs. aspiration of single-walled carbon nanotubes in C57BL/6 mice: inflammation, fibrosis, oxidative stress, and mutagenesis. Am J Physiol Lung Cell Mol Physiol 295:L552–L565.

Shvedova AA, Kisin ER, Mercer R, et al. (2005). Unusual inflammatory and fibrogenic pulmonary responses to single-walled carbon nanotubes in mice. Am J Physiol Lung Cell Mol Physiol 289:L698–L708.

Singh A, Settleman J. (2010). EMT, cancer stem cells and drug resistance: an emerging axis of evil in the war on cancer. Oncogene 29:4741–4751.

Song Y, Li X, Wang L, et al. (2011). Nanomaterials in humans: identification, characteristics, and potential damage. Toxicol Pathol 39:841–849.

Taketo MM. (2004). Shutting down Wnt signal-activated cancer. Nat Genet 36:320–322.

Tan MH, Commens CA, Burnett L, Snitch PJ. (1996). A pilot study on the percutaneous absorption of microfine titanium dioxide from sunscreens. Aust J Dermatol 37:185–187.

Thornberry NA, Lazebnik Y. (1998). Caspases: enemies within. Science 281:1312–1316.

Tucci P, Porta G, Agostini M, et al. (2013). Metabolic effects of TiO_2 nanoparticles, a common component of sunscreens and cosmetics, on human keratinocytes. Cell Death Dis 4:e549.

Turner-Warwick M. (1963). Precapillary systemic-pulmonary anastomoses. Thorax 18:225–237.

Wang L, Mercer RR, Rojanasakul Y, et al. (2010). Direct fibrogenic effects of dispersed single-walled carbon nanotubes on human lung fibroblasts. J Toxicol Environ Health A 73: 410–422.

Warheit DB, Laurence BR, Reed KL, et al. (2004). Comparative pulmonary toxicity assessment of single-wall carbon nanotubes in rats. Toxicol Sci 77:117–125.

Weir A, Westerhoff P, Fabricius L, et al. (2012). Titanium dioxide nanoparticles in food and personal care products. Environ Sci Technol 46:2242–2250.

Yoo KC, Yoon CH, Kwon D, et al. (2012). Titanium dioxide induces apoptotic cell death through reactive oxygen species-mediated Fas upregulation and Bax activation. Int J Nanomed 7:1203–1214.

Zhang AP, Sun YP. (2004). Photocatalytic killing effect of TiO_2 nanoparticles on Ls-174-t human colon carcinoma cells. World J Gastroenterol 10:3191–3193.